Servo Motor Characterization for Project Xanthus

Connor Sterling

September 2025

1 Introduction

MIT Rocket Team Project Zephyrus, among other novel design features, aims to establish active roll control of the rocket using aerodynamic control surfaces ("tabs"). The tabs are placed along the trailing edge of the fins and actuated by a thin, RC-plane grade servo. The purpose of this report is to document the efforts used to characterize the servo dynamics used on Project Xanthus, a demonstrator rocket launched in November 2025 in preparation for Zephyrus.

Section 2 provides a brief background of the project goals. Sections 3–5 outline the experimental campaign. Results and analysis are presented in Section 6.

2 Motivation

Fig. 1 depicts the block diagram governing the rocket's roll angle ϕ. K is a control gain, G is plant dynamics, H is a measurement transfer function, J_{servo} is the servo moment of inertia, τ is a torque, and α is the tab angle of attack (0° is flush with fin). A star indicates command. Dashed boxes represent digital computers. The inner transfer function α/α^* represents the servo dynamics. As the reader can see, this inner loop is complicated and contains numerous parameters that are difficult or impossible to estimate *a priori*. The goal of this campaign is to experimentally determine this transfer function to aid in control design. Ultimately, the inner loop can be dealt with explicitly, approximated as a low order system (e.g. second order), or approximated as unity. This campaign will inform that decision.

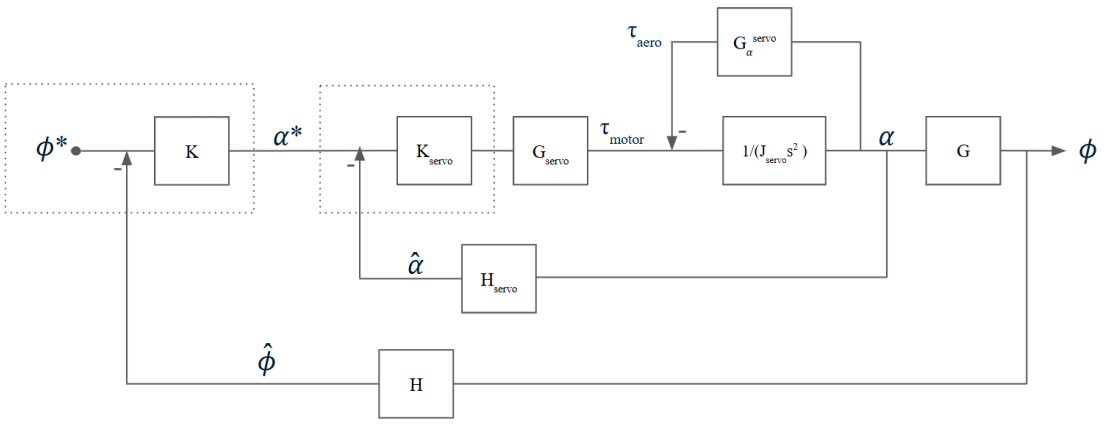

Figure 1: Roll angle block diagram.

3 Equipment

For Project Xanthus, the Zephyrus demonstrator rocket, the servos are KST X06 servos. Table 1 contains the specifications. Fig. 2 is an image of the servo. Further details can be found at [1].

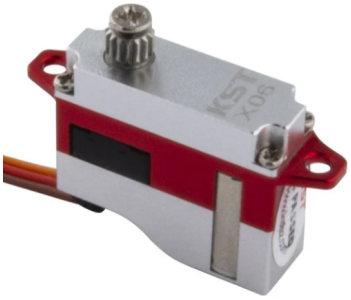

Figure 2: KST X06 servo.

Table 1: KST X06 specifications

Property	Value
Rated Voltage	DC6.0V
Voltage Range	DCV3.8V–8.4V
Rated Torque	4N-cm @ 6.0V
Rated Speed	0.20sec/60° @ 6.0V
Rated Current	0.22A @ 6.0V
Torque	0.8Kgf-cm@3.8V, 1.5Kgf-cm@ 6.0V, 1.8Kgf-cm@8.4V
Speed	0.12sec/60°@3.8V, 0.08sec/60°@6.0V, 0.07sec/60°@8.4V
Stalling Current	0.58A@ 6.0V
Default Travel Angle	±60° = 120° total travel
Operating Temperature Range	-10℃. . . . . +65℃
Case Dimensions	20mm*7mm*16.6mm±0.1mm
Weight	6g±10%
Motor Type	Coreless DC Motor
Case Material	Aluminum Alloy
Gear Set Material	Steel Gear
Position Sensor	Potentiometer
Ball Bearing	1BB

Hardware used for the experiment:

- KST X06 servo
- AS5600 magnetic encoder [2]
- Cylindrical magnet (included with AS5600)
- Arduino Mega 2560
- Digilent Analog Discover 2 (AD2)
- Kungber SPS3010 0 30 V/0 10 A power supply
- Inertia simulation mass (ISM)
- 2 X 0.12 lb/in extension spring
- 2 X 0.48 lb/in extension spring
- Encoder mount

- 2 X spring mount
- Acrylic baseplate

4 Experimental Setup

The servo is mounted to an acrylic baseplate. Affixed to the shaft is the ISM and on top of that a cylindrical magnet. The magnetic encoder is positioned above the magnet via the encoder mount. Springs are attached at one end to the inertia mount and at the other anchored to the baseplate via the spring mounts. Spring constants k and lever arm r are chosen to simulate the τ vs. α curve experienced by the servo for a given dynamic pressure. These curves are predicted using CFD. Note that $C_{L\alpha}$ =6.59 rad^{-1} predicted by CFD is close to flat plate theory. See Figs. 3–4.

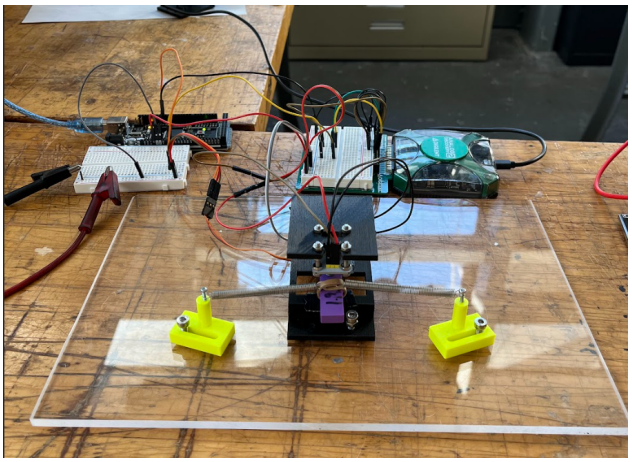

Figure 3: Experimental setup.

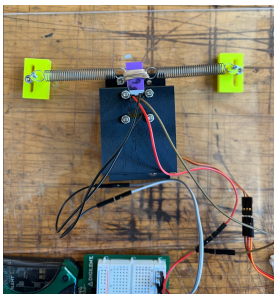

(a)

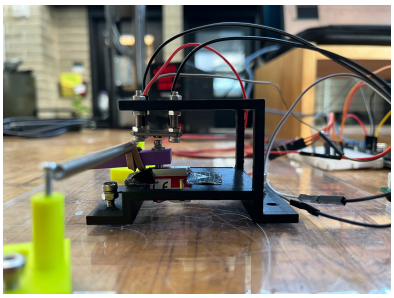

(b)

Figure 4: Experimental setup top and side views.

The servo angle command is sent from the AD2's W1 channel to Channel 1 and to the Arduino. An Arduino script maps W1 to a PWM signal corresponding to an angular range of -15° to 15° and sent to the servo. The encoder voltage output is sent to AD2 Channel 2. Bode plots are generated using the AD2's network analysis feature. The encoder is powered by the Arduino's 5 V output. The servo is powered at 6.05 V from the power supply to simulate the available voltage from the flight computer.

5 Test Matrix

The servo is tested at simulated speeds ranging from 0 m/s to 120 m/s taken at intervals of 20 m/s (seven speeds). This covers the range of predicted speeds for the Xanthus flight. A constant density of 1.17 kg/m^3

is used when calculating dynamic pressure. This is the approximate air density Xanthus is expected to see. Three trials are conducted at each speed. A trials sweep 200 mHz to 50 Hz. B trials sweep 1 Hz to 50 Hz. C trials sweep 5 Hz to 50 Hz.

6 Results and Analysis

The servo had fairly consistent performance across speeds. Above roughly 22.5 Hz, the motor begins to "alias". Response amplitude drops, before growing in magnitude but at a slower frequency than commanded as f approaches 50 Hz. Voltage from the power supply also fluctuates rapidly, ranging from below 5 V to 6.05 V. For this reason, data above 22.5 Hz are not reported or considered in the analysis. Data from A and B trials are interpolated to a common frequency axis for the fitting analysis.

A transfer function of the following form is sought:

$$G_{servo}^{CL} = \frac{b_m s^m + b_{m-1} s^{m-1} + ... + b_1 s + b_0}{a_n s^n + a_{n-1} s^{n-1} + ... + a_1 s + a_0}. \tag{1}$$

For clarity, the transfer function is hereafter referred to simply as G. Three nonlinear fits are attempted to create a transfer function that replicates the frequency response of the servo: a) second-order denominator and zeroth-order numerator (N2M0), b) second-order denominator and first-order numerator (N2M1), and c) third-order numerator and second-order denominator (N3M2). For any fit, $n > m$ must be true or gain magnitude will not vanish at high frequencies. An "N3M1" model is not chosen because the difference $n-m$ is consequential in system dynamics (as can be readily seen under root locus analysis). Additionally, the constraint $a_0 = b_0$ is enforced to ensure that gain asymptotes to unity at low frequencies.

The problem is posed as an unconstrained optimization for $n + m + 1$ parameters. The cost function minimizes squared error of the complex gain. It is weighted by proximity to the resonant frequency according to a Gaussian distribution normalized to a range of 0 to 1. This is to best capture behavior in the region around the resonant frequency and subsequent attenuation and limit influence of the low frequency region where $|G| \approx 1$. The cost function is reproduced below:

$$J = |G_{experimental} - G_{model}|^2 \cdot \frac{H(\omega)}{\max_i \left(H(\omega_i)\right)}, \tag{2}$$

where

$$H(\omega) = \exp\left(-0.5 \cdot \frac{(\omega - \omega_r)^2}{(\omega_r/3)^2}\right).$$

Figures 5-7 present the curve fits in order of increasing parameter number.

Clearly, a simple second-order approximation does not capture the system dynamics. This could be anticipated, as $n - m = 2$, which does not reflect the real system. The introduction of a single zero produces a much better fit. The N3M2 model yields a near perfect fit for frequencies until around the bandwidth, where the phase loss is under-predicted slightly. Note that the latter represents a system of equivalent order to the analytic model.

A pole-zero analysis produces interesting results. Tabs. 2 and 3 contain the fitted poles and zeros for N2M1 and N3M2, respectively. Tabs. 4 and 5 contain the model coefficients. Interestingly, for the 20 m/s and 40 m/s case, the optimization reduces the N3M2 model to equivalence with an N2M1 model. In this case, the coefficients suggest an instability since they fail to meet the necessary condition $a_i > 0 \ \forall i$ for stability. Further work on the optimization algorithm could be done to correct the degenerate fit, but was deemed not worth the effort.

For the purposes of control, it was originally hypothesized that an N2M1 approximation is sufficient for controller design. The frequency response can be closely replicated with this model, and pole-zero analysis shows that phase contributions around the targeted CL poles for performance are similar when conducting a root-locus design. Eventually, it was determined that using the full model is best practice, as it adds little complexity to the design process with the use of numerical tools and can alter the root locus.

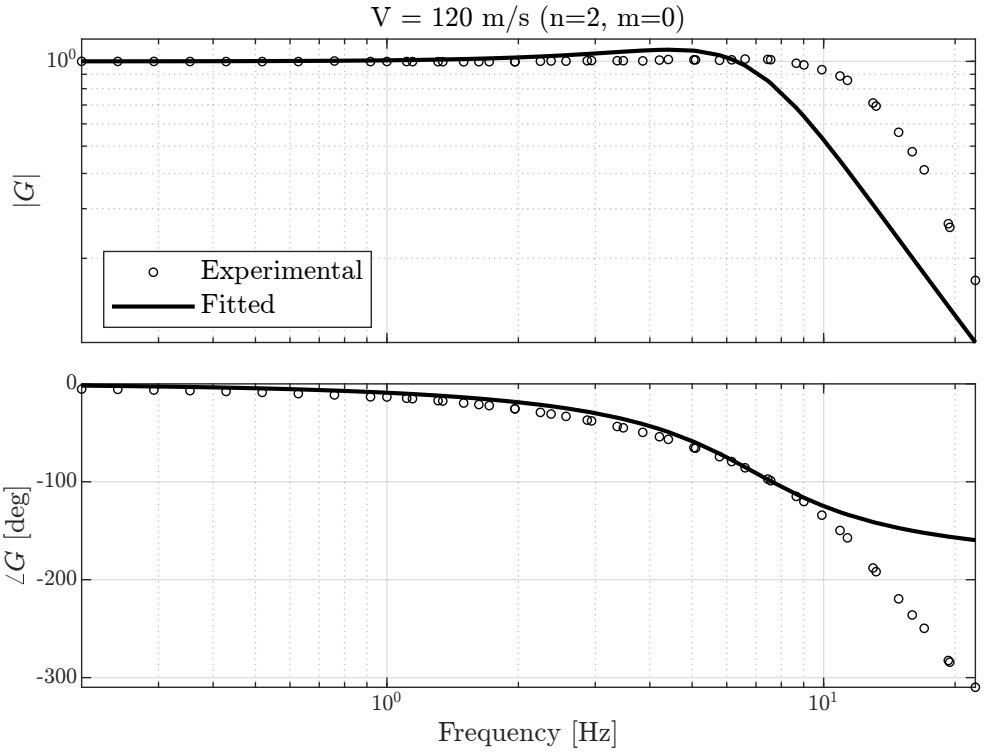

Figure 5: Curve fit for $n = 2, m = 0$ at 120 m/s.

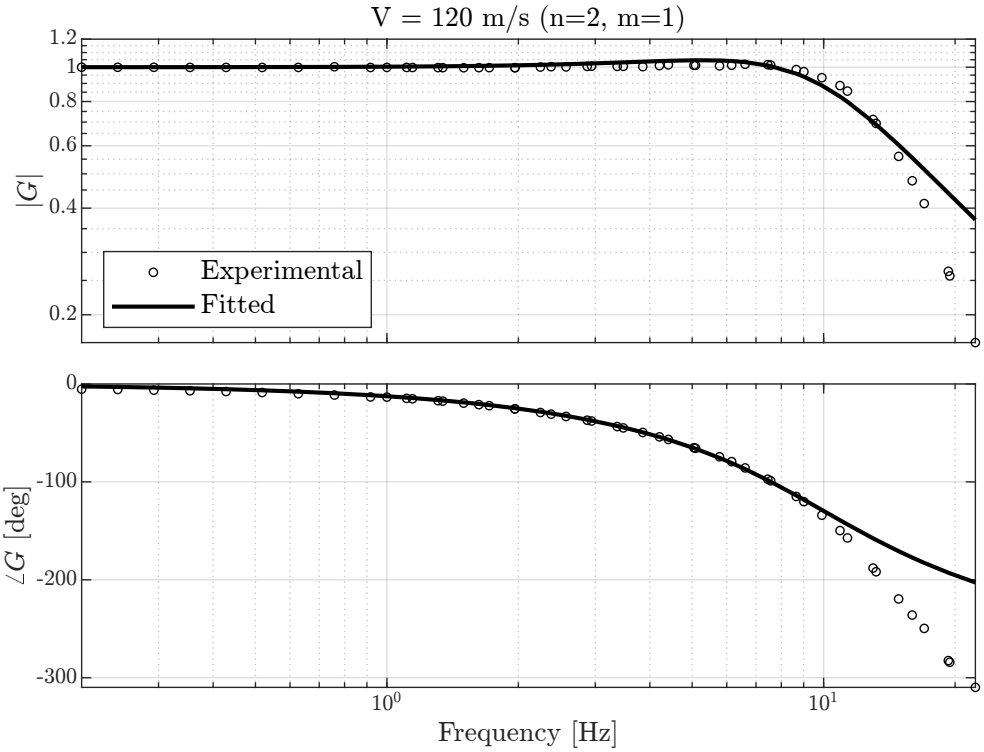

Figure 6: Curve fit for $n = 2, m = 1$ at 120 m/s.

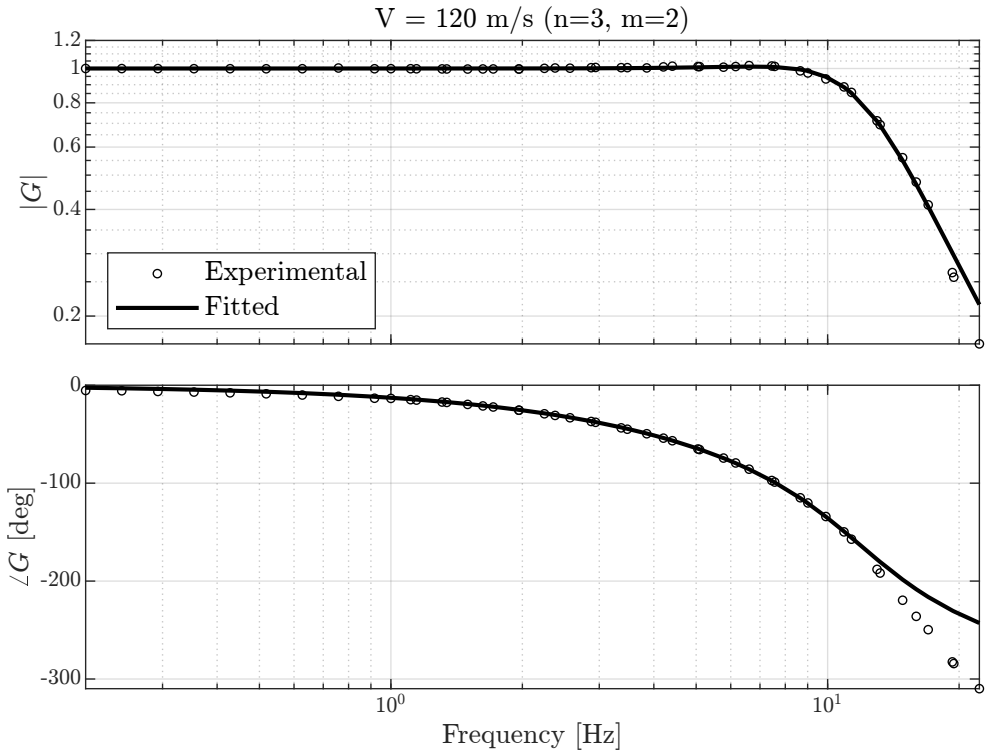

Figure 7: Curve fit for $n = 3, m = 2$ at 120 m/s.

A Tabulated poles, zeros, and coefficients

Table 2: Poles and zeros for $n = 2, m = 1$

V [m/s]	$p_{1,2}$	z_1
0	$-41.10 \pm 43.01j$	83.58
20	$-44.45 \pm 41.63j$	82.44
40	$-48.88 \pm 41.29j$	79.19
60	$-43.12 \pm 42.12j$	83.41
80	$-42.46 \pm 43.49j$	82.03
100	$-43.93 \pm 43.57j$	80.17
120	$-42.18 \pm 44.13j$	82.61
Mean	$-43.73 \pm 42.75j$	81.92
S.D.	2.75	1.65

Table 3: Poles and zeros for $n = 3, m = 2$

V [m/s]	$p_{1,2}$	p_3	z_1	z_2
0	$-34.59 \pm 58.41j$	-57.10	-155.72	103.00
20	$-43.28 \pm 42.51j$	0.01	80.72	0.01
40	$-47.97 \pm 42.00j$	0.01	78.08	0.01
60	$-34.94 \pm 59.64j$	-53.41	-151.89	103.79
80	$-34.32 \pm 61.56j$	-54.48	-168.75	102.62
100	$-34.11 \pm 61.52j$	-50.74	-134.50	97.19
120	$-35.27 \pm 66.03j$	-59.78	-396.69	114.71
Mean[1]	$-34.65 \pm 61.43j$	-55.10	-201.51	104.26
S.D.[1]	2.93	3.47	109.79	6.40

[1] 20 m/s and 40 m/s values omitted from calculation.

Table 4: N2M1 coefficients

Speed [m/s]	a_0	a_1	a_2	b_0	b_1
0	7.755	180.1	2.191	7755	-92.79
20	7.761	186.0	2.093	7761	-94.14
40	7.694	183.7	1.879	7694	-97.16
60	7.765	184.3	2.137	7765	-93.08
80	7.722	177.5	2.090	7722	-94.14
100	7.690	176.5	2.009	7690	-95.92
120	7.723	174.8	2.073	7723	-93.49
Mean	7.730	180.4	2.068	7730	-94.34
S.D.	31.09	4.330	.1001	31.09	1.592

Table 5: N3M2 coefficients

Speed [m/s]	a_0	a_1	a_2	a_3	b_0	b_1	b_2
0	364400	11854	174.9	1.385	364.4	-1198	-22.72
20	-28.73	4804	113.0	1.305	-28.73	4730	-58.59
40	-28.10	4787	113.0	1.178	-28.10	4748	-60.81
60	356300	11882	172.1	1.396	356300	-1087	-22.60
80	405200	13036	184.3	1.497	405200	-1548	-23.40
100	368400	12338	174.5	1.467	368400	-1051	-28.18
120	523700	15353	203.7	1.563	523700	-3245	-11.51
Mean[1]	403600	12892	181.9	1.462	403600	-1626	-21.68
S.D.[1]	69730	1456	13.05	0.07382	69730	926.4	6.136

[1] 20 m/s and 40 m/s values omitted from calculation.

References

[1] KST Servos, "X06 V6.0 HV Micro Digital Metal Gear Glider 1.8kg Torque Servo Motor," 2025, accessed: 2025-09-17. [Online]. Available: https://kstservos.com/products/x06-v6-0-hv-micro-digital-metal-gear-glider-1-8kg-torque-servo-motor

[2] AMS OSRAM, *AS5600 12-bit Programmable Contactless Potentiometer Operation Manual*, Dec. 2014, accessed: 2025-09-17. [Online]. Available: https://look.ams-osram.com/m/4f8342513a447495/original/AS5600_UG000254_2-00.pdf